Analytical and Bioanalytical Chemistry (2021) 413:3369–3379
https://doi.org/10.1007/s00216-021-03278-8

RESEARCH PAPER

# Drop-of-blood acoustic tweezing technique for integrative turbidimetric and elastometric measurement of blood coagulation

Daishen Luo[1] · Erika M. Chelales[1] · Millicent M. Beard[1] · Nithya Kasireddy[1] · Damir B. Khismatullin[1]

Received: 29 October 2020 / Revised: 25 February 2021 / Accepted: 4 March 2021 / Published online: 1 April 2021


## Abstract

Many patients develop coagulation abnormalities due to chronic and hereditary disorders, infectious disease, blood loss, extracorporeal circulation, and oral anticoagulant misuse. These abnormalities lead to bleeding or thrombotic complications, the risk of which is assessed by coagulation analysis. Current coagulation tests pose safety concerns for neonates and small children due to large sample volume requirement and may be unreliable for patients with coagulopathy. This study introduces a containerless drop-of-blood method for coagulation analysis, termed "integrated quasi-static acoustic tweezing thromboelastometry" (i-QATT™), that addresses these needs. In i-QATT™, a single drop of blood is forced to levitate and deform by the acoustic radiation force. Coagulation-induced changes in drop turbidity and firmness are measured simultaneously at different instants. The parameters describing early, intermediate, and late stages of the coagulation process are evaluated from the resulting graphical outputs. i-QATT™ rapidly (<10 min) detected hyper- and hypo-coagulable states and identified single deficiency in coagulation factors VII, VIII, IX, X, and XIII. The linear relationship ($r^2 > 0.9$) was established between fibrinogen concentration and two i-QATT™ parameters: maximum clot firmness and maximum fibrin level. Factor XIII activity was uniquely measured by the fibrin network formation time ($r^2 = 0.9$). Reaction time, fibrin formation rate, and time to firm clot formation were linearly correlated with heparin concentration ($r^2 > 0.7$). tPA-induced hyperfibrinolysis was detected in the clot firmness output at 10 min. i-QATT™ provides comprehensive coagulation analysis in point-of-care or laboratory settings, well suited to the needs of neonatal and pediatric patients and adult patients with anemia or blood collection issues.

**Keywords** Coagulation analysis · Coagulation factors · Anticoagulants · Fibrinolysis · Pediatrics

## Introduction

Plasma and whole-blood coagulation tests are routinely performed to assess bleeding and thrombosis risks in critical care patients [1, 2], patients with coagulation disorders [3, 4], and patients on anticoagulant therapy [5]. Using a photo-optical turbidimetric or nephelometric technique [6, 7], plasma tests predict the onset of fibrin formation (reaction time) upon exposure to activators of extrinsic (PT/INR) or intrinsic pathway of coagulation (aPTT). The information about later stages, which is essential for bleeding/thrombotic risk prediction, can be obtained from whole-blood elastometric tests (TEG or ROTEM) in which temporal changes in blood elasticity (firmness) are measured [8, 9]. However, both TEG and ROTEM require frequent calibration, have high variability, and are not standardized for coagulation measurements [8, 10, 11].

The available coagulation analyzers operate with a relatively large sample volume, thus wasting this precious resource. Two to three milliliters of blood collected for one set of coagulation tests is a significant amount for neonates and small children [12]. With multiple tests performed at relatively short time intervals, pediatric patients may lose too much blood and become anemic. Due to a lack of clinically validated devices that can operate with small blood samples, monitoring of coagulation abnormalities in small children remains challenging [13, 14].

There also is a growing concern that coagulation tests are unreliable [15], particularly, in coagulopathic and thrombotic patients [8, 10, 13, 16, 17]. Diagnostic errors can be caused by

✉ Damir B. Khismatullin
damir@tulane.edu

[1] Department of Biomedical Engineering and Tulane Institute for Integrative Engineering for Health and Medicine, Tulane University, 6823 St. Charles Avenue 500 Lindy Boggs Center, New Orleans, LA 70118, USA

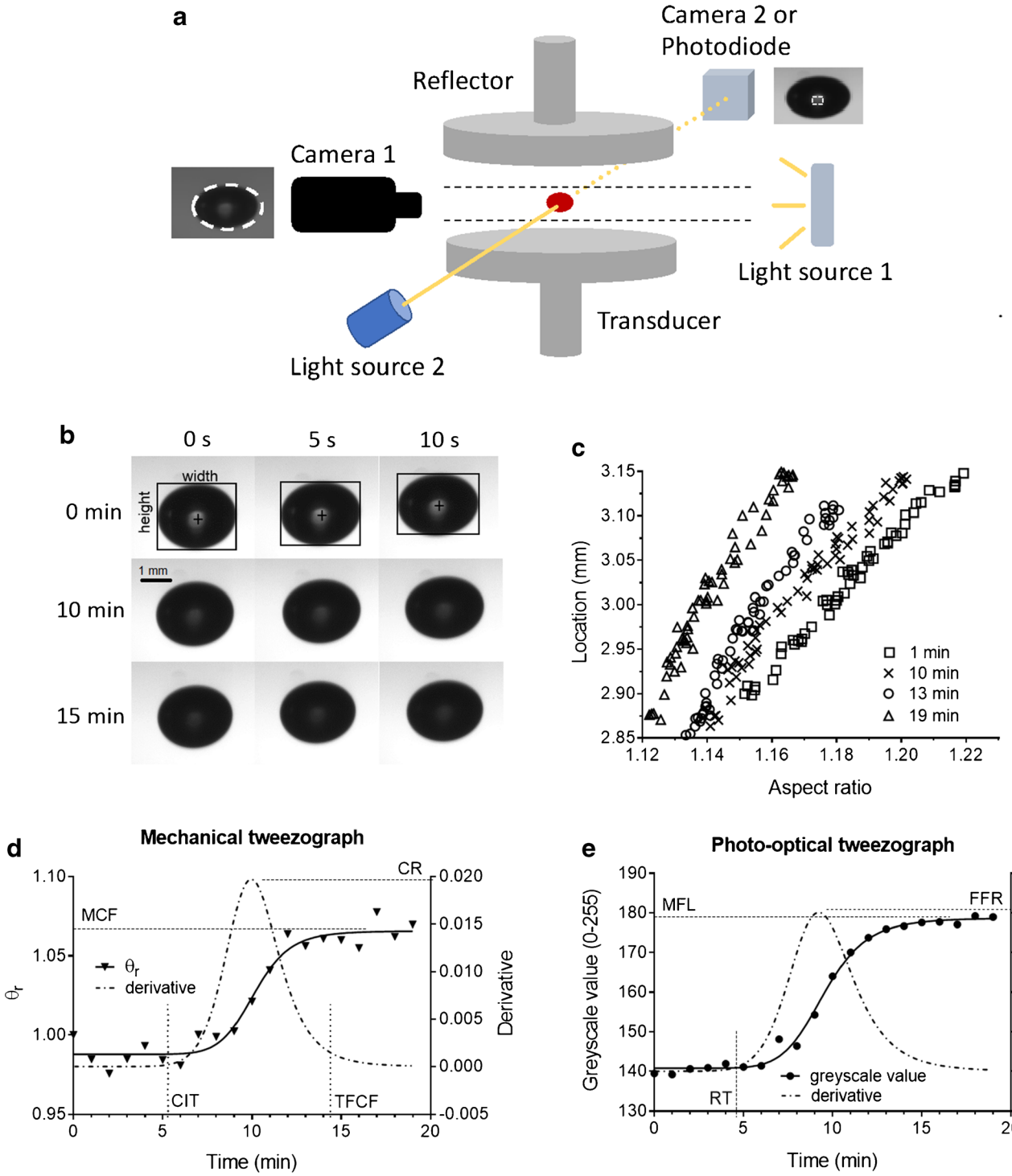


**Fig. 1** Quasi-static acoustic tweezing thromboelastometry (QATT) integrated with photo-optical turbidimetry. Shown are **a** schematic diagram of the experimental system: the shape of a levitated blood drop is recorded by camera 1 and blood turbidity is measured from light intensity in the central square region of the drop recorded by camera 2 or photodiode; **b** photographs of an acoustically levitated and deformed (acoustically tweezed) sample drop of normal blood plasma before the onset of coagulation (0 min), during coagulation (10 min), and when plasma is fully clotted (15 min); **c** location vs. aspect ratio curves for a sample drop of normal blood plasma at 1, 10, 13, and 19 min of sample tweezing; **d** mechanical tweezograph (elasticity vs. time curve) for coagulating normal blood plasma; and **e** photo-optical tweezograph (darkness in greyscale value vs. time) for coagulating normal blood plasma. Blood plasma was exposed to an intrinsic pathway activator (APTT-XL) and calcium chloride. The columns in **b** and symbols in **c** are the data collected during the deformation phase of the pressure sweep

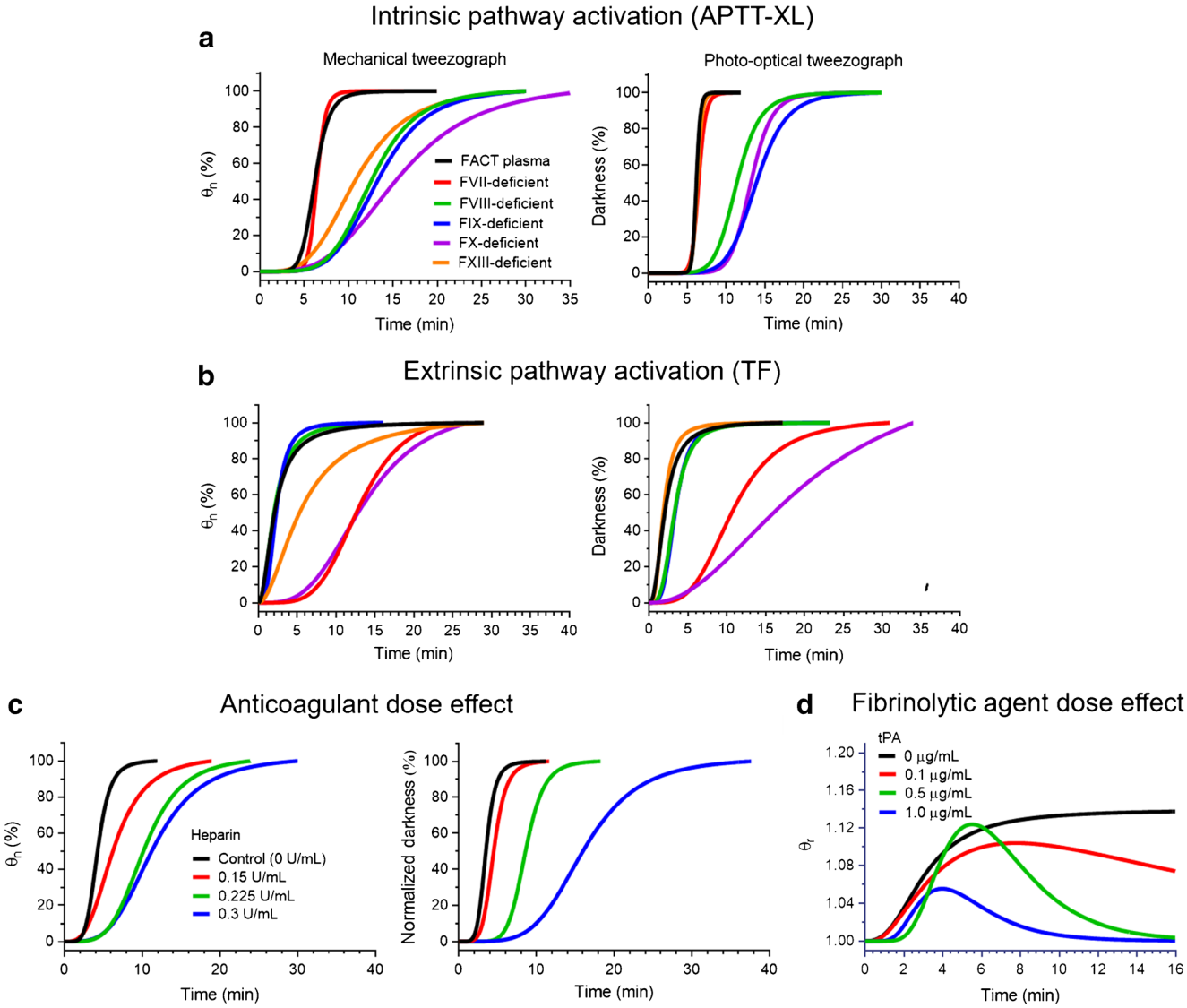


**Fig. 2** Graphical output of i-QATT™. **a**, **b** Shown are the mechanical (left) and photo-optical tweezographs (right) of 3–4 drops of normal blood plasma (FACT) and factor-deficient plasmas exposed to an intrinsic (APTT-XL, **a**) or extrinsic (TF, **b**) pathway activator. **c** Mechanical and photo-optical tweezographs of normal blood plasma exposed to heparin at different doses (4–7 samples per dose) and then activated via the extrinsic pathway. **d** Mechanical tweezographs of normal blood plasma exposed to fibrinolytic agent tPA at different doses (5 samples per dose) and then activated via the extrinsic pathway

direct contact of a blood sample with artificial materials, e.g., container or cartridge walls, during coagulation. Blood is a very sensitive biological material, and its coagulation in the body is triggered by activated endothelial cells, collagen, and/or external environment such as air. When it is exposed to artificial materials, improper changes in this process may occur.

We have developed acoustic tweezing technology that addresses the issues of sample size and sample-wall contact in coagulation analysis [18, 19]. In our approach, temporal changes in blood viscoelasticity during coagulation are assessed from a single drop of blood (4–6 μL in volume) levitated and deformed in air in a standing acoustic wave field. Simultaneously with this mechanical measurement, we measure changes in blood turbidity from acquired images of the blood drop. The focus of this study is to assess the feasibility of this integrated quasi-static technique (i-QATT™) to detect coagulation factor deficiency, measure functional levels of coagulation factors and fibrinolytic agents, and monitor anticoagulant therapy.

## Materials and methods

**Reagents** Pacific Hemostasis® PT (Thromboplastin-D) and aPTT reagents (aPTT-XL) were purchased from Fisher Scientific (Hampton, NH). Thromboplastin-D was suspended in 4 mL PBS. Calcium chloride, porcine heparin sodium, and

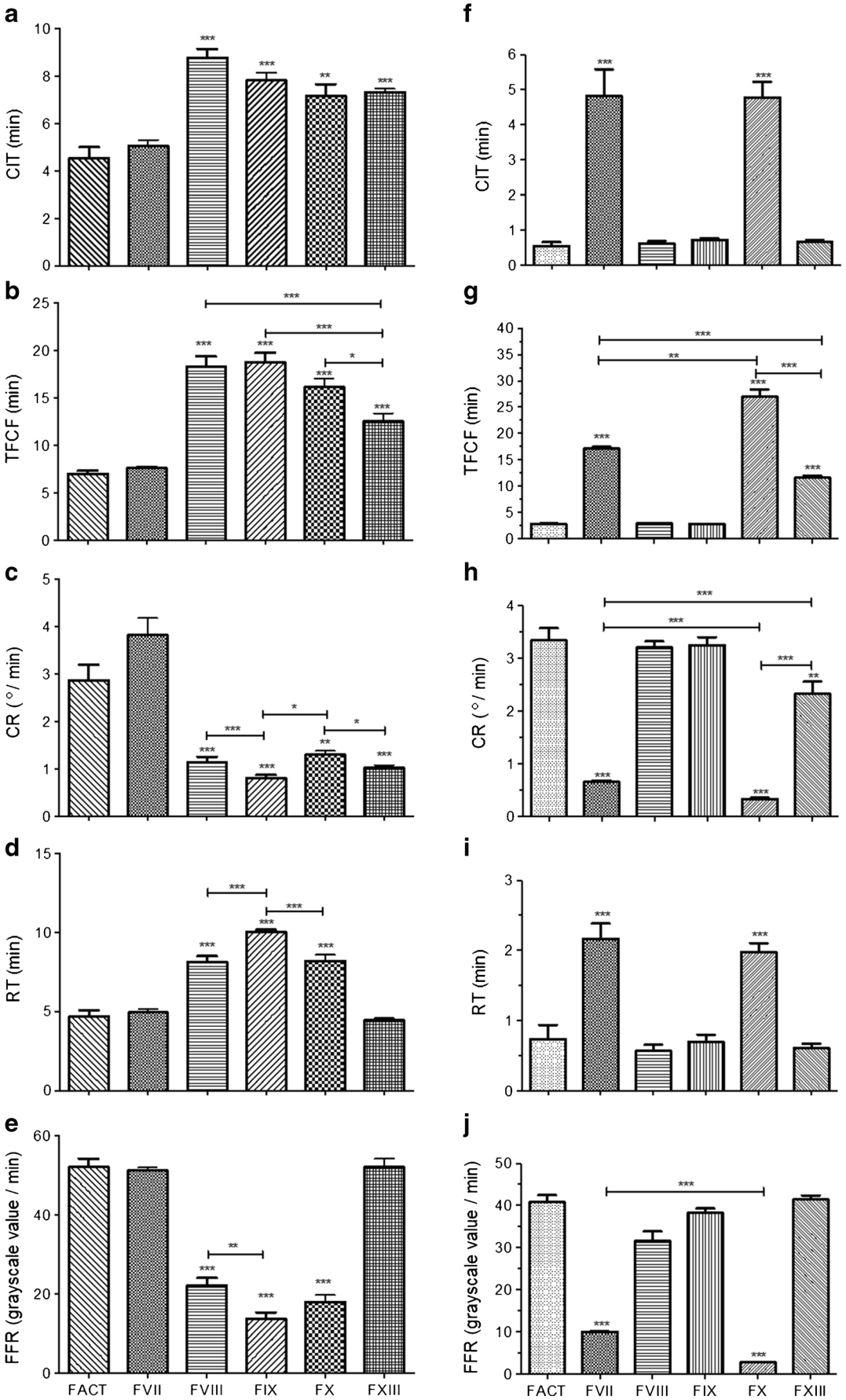
a
CIT (min)
b
TFCF (min)
c
CR (°/ min)
d
RT (min)
e
FFR (grayscale value / min)
FACT
FVII
FVIII
FIX
FX
FXIII
f
CIT (min)
g
TFCF (min)
h
CR (°/ min)
i
RT (min)
j
FFR (grayscale value / min)
FACT
FVII
FVIII
FIX
FX
FXIII

◀ **Fig. 3** i-QATT™ measurement of factor-deficient plasma activated through either the intrinsic pathway (left panel) or the extrinsic pathway (right panel). The values of coagulation parameters CIT (**a**, **f**), TFCF (**b**, **g**), CR (**c**, **h**), RT (**d**, **i**), and FFR (**e**, **j**) for normal and factor-deficient plasmas, extracted from the tweezographs. Mean ± SEM of 4 independent tests. $*p < 0.05$, $**p < 0.01$, $***p < 0.001$

human tissue plasminogen activator (tPA) were obtained from Sigma-Aldrich (St. Louis, MO). Calcium chloride was dissolved in deionized water at a 222 mg/mL concentration (2 M). Heparin sodium was diluted in PBS into a 13.5 KU/mL stock solution. The tPA stock solution was prepared by dissolving tPA into PBS at a 0.5 mg/mL concentration. Human fibrinogen solution was purchased from Enzyme Research Laboratories (South Bend, IN) and diluted in PBS into a 400 mg/mL stock solution.

**Blood plasma preparation** FACT plasma and plasmas with deficiency in FVII, FVIII, FIX, FX, and FXIII (less than 1% activity) were purchased from George King Bio-Medical (Overland Park, KA). Low fibrinogen-level plasma was purchased from Fisher Scientific (Hampton, NH). The extrinsic and intrinsic pathways of coagulation were triggered by thromboplastin-D (where TF is an active ingredient) and aPTT-XL, respectively, following either manufacturer's instructions ("commercial recipe") or a custom recipe. The data produced using the commercial recipe are discussed in Supplementary Information (ESM) (see Supplementary Methods and Results) and shown in ESM Figs. S2 and S3. In the custom recipe, 2 mL thromboplastin-D was mixed with 18 mL of blood plasma to activate the extrinsic pathway. Six milliliters aPTT-XL and 2 mL calcium chloride were added to 18 mL blood plasma to activate the intrinsic pathway.

In the fibrinogen study, a batch of FACT plasma with 295 mg/dL fibrinogen concentration, as measured by Clauss' method, was used as a base. One hundred eighty microliters plasma was mixed with 20 μL of either PBS or fibrinogen-in-PBS solution to reach the final fibrinogen concentration of 265, 300, 400, 500, or 600 mg/dL. Low fibrinogen plasma (70 mg/dL) was also used in this study.

To test the impact of heparin on blood coagulation, 200 μL FACT plasma was mixed with 20 μL PBS or heparin-in-PBS to achieve the final heparin concentration of 0, 0.15, 0.225, 0.3, or 0.6 U/mL. After 15-min incubation, the thromboplastin-D solution prepared by the custom recipe was applied to a heparin-treated plasma sample to activate the coagulation process. This procedure was similar to the Rapid TEG test [20]. The effect of FXIII activity on blood coagulation was measured using normal (100% activity), FXIII-deficient plasma (<1%), and a 1:1 mixture of normal and FXIII-deficient plasmas (50%).

**Experimental system** The acoustic tweezing coagulometer [18] consists of the following: (1) a custom Langevin-type acoustic transducer; (2) a reflector mounted at full wavelength away from the transducer; (3) a function synthesizer (Agilent 33220A, Santa Clara, CA) and a wideband power amplifier (Krohn-Hite 7500, Brockton, MA) that generate the driving signal at a frequency of 29.4 kHz; (4) two backlit light boxes and two CMOS camera (acA1920-25um, Basler, Ahrensburg, Germany) to record drop images; (5) an electronic single-channel pipette (CappMaestro, Capp, Nordhausen, Germany) for semi-automatic sample handling; and (6) a custom environmental chamber integrated with a humidifier that maintains humidity at 90%. The coagulometer is controlled by a computer workstation connected to the function generator and the cameras. The device is 40 cm long, 30 cm wide, and 20 cm high, i.e., it is small enough to be placed on bedside.

In i-QATT™ analysis (Fig. 1a, see also ESM Fig. S1), a 6-μL blood drop was injected into the standing wave field by the pipette. The drop was first maintained at an aspect ratio close to 1, referred to as a "resting state." This was achieved when the input power of the transducer was 3.9 W. Quasi-static acoustic tweezing of the drop was induced through a series of 1-min pressure sweeps. In each sweep, the input voltage (and thus the acoustic pressure) increased at a fixed increment for 15 s to deform the drop to a maximum aspect ratio of ~2.2 and then dropped to its resting state in 5 s. The resting state was maintained for 40 s, i.e., until the next pressure sweep began. Changes in the drop aspect ratio (applied strain measure), drop vertical location (measure of the applied extensional strain), and drop light transparency were assessed from recorded images of the drop (Fig. 1b). It is important to say that the drop vertical position in the resting state is below a pressure node because of gravity. An increase in acoustic pressure causes the drop to move to a higher location, closer to the node, and it also induces vertical contraction of the drop, resulting in an increase in drop aspect ratio.

**Data analysis** By using a custom image analysis code, we first plotted drop aspect ratio vs. location at different instances (Fig. 1c). Please note that times reported there are pressure sweep numbers, converted to the time scale based on the fact that the sweep duration is 1 min. The linear part of the aspect ratio vs. location curves was used to determine the slope angle $\theta$ (a measure of sample firmness), which was then converted into the relative angle.

$$\theta_r = \theta/\theta_0 \tag{1}$$

or the normalized angle

$$\theta_n = \frac{\theta_r - 1}{\theta_{r,\max} - 1} \times 100\% \tag{2}$$

where $\theta_0$ is the initial angle and $\theta_{r,max}$ is the maximum value of $\theta_r$. The set of time plots of $\theta_r$ andd $\theta_n$ and their derivatives is the i-QATT™ graphical output for blood firmness changes, referred to as a "mechanical tweezograph" (Fig. 1d). Simultaneously with

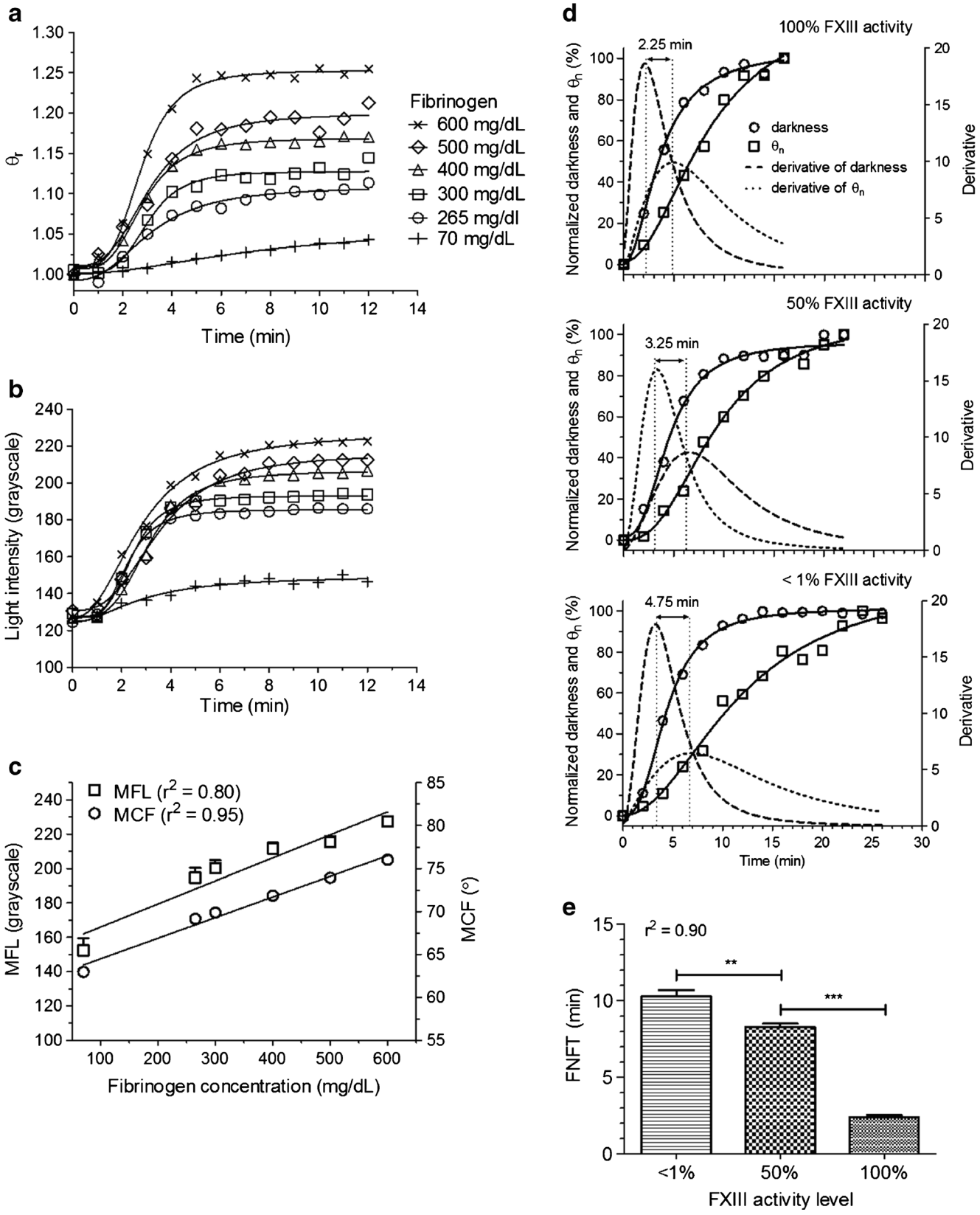


drop shape analysis, we measured changes in light intensity in the center of the drop (20 pixels × 20 pixels area), which provided us with the graphical output for fibrin formation kinetics ("photo-optical tweezograph," Fig. 1e). The light intensity was measured

◀ **Fig. 4** Effect of fibrinogen and factor XIII on blood plasma coagulation as assessed by i-QATT™. Shown are **a** mechanical and **b** photo-optical tweezographs for normal plasma reconstituted with fibrinogen at a final concentration of 70–600 mg/dL. **c** The coagulation parameters MFL and MCF show a linear dependence on fibrinogen concentration. **d** Time delay between mechanical and photo-optical tweezing data for blood plasma with different levels of FXIII activity (100%, 50%, and <1% of the normal level). **e** The effect of FXIII on coagulation parameter FNFT. Mean ± SEM of 5–7 independent tests. $*p < 0.05$, $**p < 0.01$, $***p < 0.001$

in grayscale values (0–255). Darkness was defined as a grayscale value divided by 255. Normalized darkness was calculated from Eq. (2) by replacing the angle with the light intensity.

**i-QATT™ parameters** The following coagulation parameters were obtained from sigmoidal fitting of tweezographs: (1) CIT, the onset time of blood firmness change; (2) TFCF, the time when blood firmness reaches its plateau value; (3) CR, the maximum rate of firmness change; (4) LY10 or LY15, blood firmness at 10 or 15 min; (5) MCF, the plateau value of blood firmness; (6) RT, the onset time of light intensity change; (7) FFR, the maximum rate of light intensity change; (8) MFL, the plateau value of the light intensity; and (9) FNFT, the difference between TFCF and RT.

**Statistical analysis** Statistical analysis of coagulation parameter values was conducted using GraphPad Prism (GraphPad Software, La Jolla, CA). The data were presented as mean ± SEM. The sample size was five or larger. The $p$ value was calculated by two-tailed, unpaired $t$-test and set at <0.05 for a statistically significant difference.

## Results

**Mechanical and photo-optical tweezographs** As seen in Fig. 2a, the mechanical tweezographs for normal and FVII-deficient plasmas (black and red lines) activated by APTT-XL were nearly identical, while plasmas with FVIII (green), FIX (blue), FX (purple), or FXIII deficiency (orange) showed prolonged coagulation. In the photo-optical tweezographs, prolonged coagulation was observed in FVIII-, FIX-, and FX- but not FXIII-deficient plasmas. These differences are due to factor deficiency in the intrinsic pathway (FVIII, FIX) and the downstream common pathway (FX, FXIII; see ESM Fig. S5). FXIII deficiency was detected in only the mechanical tweezograph for the following reason. FXIII is the final enzyme in the coagulation cascade that cross-links fibrin molecules formed during early stages of this process. It has no effect on fibrin formation. Fibrin cross-linking leads to an increase in clot firmness until the clot reaches its mature state, which is what the mechanical tweezograph exactly measures. i-QATT™ accurately predicted defects in the extrinsic pathway, as evident by prolonged coagulation of thromboplastin-D- (TF-) but not APTT-XL-activated FVII-deficient plasmas (Fig. 2b vs. a). As expected, there was a strong delay in the coagulation process for TF-activated plasmas deficient in FX or FXIII and normal coagulation for plasmas deficient in FVIII or FIX (Fig. 2b).

Figure 2c shows i-QATT™ measurement of blood plasma coagulation at a clinical range of heparin concentration (0–0.6 U/mL) [21, 22]. Both mechanical and photo-optical data demonstrated that the coagulation became more prolonged with an increase in heparin dose. i-QATT™ captures tPA-induced fibrinolysis, as seen in Fig. 2d. The firmness of a tweezed blood plasma drop was reduced to its initial value within 14 min at tPA dose of 0.5 μg/mL or higher. Additionally, i-QATT™ whole-blood analysis indicates prolonged coagulation and a reduction in clot firmness with high doses of heparin and complete fibrinolysis at 15 to 20 min for 0.5 μg/mL tPA (ESM Fig. S4).

**Coagulation factor deficiency detection** The values of five coagulation parameters (CIT, TFCF, CR, RT, and FFR) extracted from mechanical and photo-optical tweezographs of plasma samples are seen in Fig. 3 and ESM Table S1. Each of the parameters demonstrated sensitivity to factor deficiency. In the case of the intrinsic pathway activation, CIT significantly increased from its normal value (4.6 ± 0.45 min) to 8.8 ± 1.0 min for FVIII-, 7.8 ± 0.96 min for FIX-, 7.2 ± 0.49 min for FX-, and 7.3 ± 0.14 min for FXIII-deficient plasmas (Fig. 3a). TFCF for FXIII-deficient plasma (13 ± 0.84 min) was significantly higher than that for normal plasma (7.0 ± 0.31 min) and significantly lower than that for FVIII- (1.1 ± 0.12 min), FIX- (19 ± 0.99 min), or FX-deficient plasma (16 ± 0.90 min) (Fig. 3b). Thus, TFCF can be used to rule out whether blood plasma has a single deficiency in FXIII. FIX deficiency can be detected from CR, RT, and FFR values (Fig. 3c–e). Specifically, CR for FIX-deficient plasma (0.80 ± 0.07°/min) was significantly lower than that for normal (2.9 ± 0.33°/min), FVIII-deficient (1.14 ± 0.12°/min), or FX-deficient plasma (0.80 ± 0.07°/min) (Fig. 3c). RT significantly increased from its normal value (4.7 ± 0.40 min) to 8.2 ± 0.36 min and 8.2 ± 0.39 min for plasma deficient in FVIII and FX, respectively, and further prolonged to 10 ± 0.15 min for FIX-deficient plasma. FFR was 53 ± 4.2 $min^{-1}$ for normal plasma but dropped to 22 ± 2.0 $min^{-1}$ with FVIII deficiency or 18 ± 1.7 $min^{-1}$ with FX deficiency. It reached its lowest value of 14 ± 1.6 $min^{-1}$ for plasma deficient in FIX. Note that CIT was much higher than RT for FXIII-deficient plasma (cf. Figure 3a and d) because of the prolonged fibrin cross-linking time.

With extrinsic pathway activation, CIT elevated from 0.55 ± 0.11 min to 4.8 ± 0.75 min or 4.8 ± 0.43 min in plasmas with FVII or FX deficiency, respectively (8.7 times higher than the

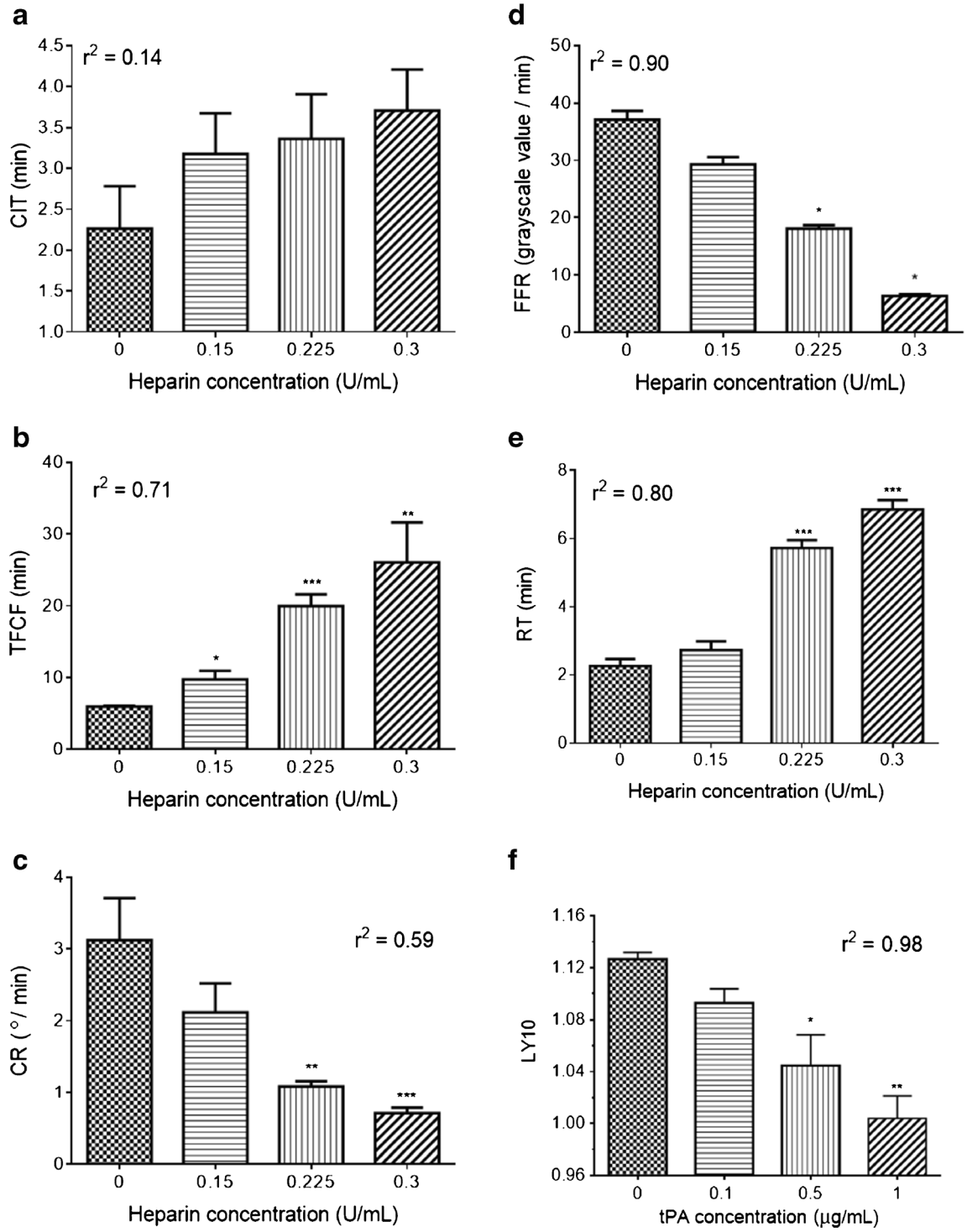


**Fig. 5** Dose effect of heparin and tPA on blood plasma coagulation, as assessed by i-QATT™. The values of coagulation parameters CIT (**a**), TFCF (**b**), CR (**c**), RT (**d**), and FFR (**e**) for control and heparin-treated plasma and LY10 (**f**) for tPA treated plasma. Mean ± SEM of 4 independent tests. *$p < 0.05$, **$p < 0.01$, ***$p < 0.001$

normal value; Fig. 3f). Note that APTT-XL elevated the CIT by 1.6 times in those plasma samples (Fig. 3a). This result points out that i-QATT™ is highly sensitive to deficiencies in FX and other common pathway factors when anticoagulated blood samples are activated via the extrinsic pathway. Deficiency in FVII, FXIII, or FX had a significant effect on TFCF and CR of TF-activated plasma. Particularly, TFCF rose from the normal plasma value (2.8 ± 0.10 min) to 12 ± 0.40 min for FXIII-, 17 ± 0.36 min for FVII-, and 27 ± 1.4 min for FX-deficient plasmas (Fig. 3g). Normal plasma

CR was 3.3 ± 0.23°/min, while FXIII-, FVII-, and FX-deficient plasmas had much lower values: 2.3 ± 0.24°/min, 0.66 ± 0.02°/min, and 0.33 ± 0.02°/min, respectively (Fig. 3h). Therefore, the TFCF or CR data can be used to rule out single factor deficiency in FVII and FXIII and to detect FX deficiency. RT was much slower in FVII- (2.2 ± 0.22 min) and FX-deficient plasma (2.0 ± 0.13 min) than in normal plasma (0.74 ± 0.20 min) or plasma with deficiency in other factors (Fig. 3i). FFR also showed sensitivity to FVII and FX deficiencies (normal: 41 ± 2.7 $min^{-1}$, FVII: 10 ± 0.31 $min^{-1}$, and FX: 2.8 ± 0.12 $min^{-1}$; Fig. 3j).

**Measurement of functional levels of fibrinogen and FXIII** During the initial stage of coagulation, the fibrin concentration increases until reaching a plateau that uniquely depends on its initial concentration [23]. The photo-optical tweezograph provided the information about how the fibrin level changed over time, with the plateau value referred to as MFL (Fig. 1d). Similarly, in the mechanical tweezograph, clot firmness reached its plateau value (MCF) at the final stage of clotting (Fig. 1c), which is highly correlated with fibrinogen concentration [24]. Figure 4a–c demonstrate that plasma MCF and MFL values were linearly correlated ($r^2 \geq 0.8$) with fibrinogen concentration ranged from 70 to 600 mg/dL. Within this range, MCF and MFL increased from 1.05 ± 0.01 to 1.3 ± 0.02 and from 127 ± 5.8 to 227 ± 2.5, respectively.

By integrating photo-optical and mechanical data, we can measure the time for fibrin cross-linking. This parameter, referred to as fibrin network formation time (FNFT), is a function of FXIII activity, a major fibrin cross-linker. As seen in Fig. 4d, FNFT significantly increased from its normal plasma value (2.4 ± 0.11 min, 100% FXIII activity) to 8.3 ± 0.21 min and 10.3 ± 0.39 min for plasmas with 50% and < 1% FXIII activity, respectively. FNFT had a strong linear correlation with FXIII activity level ($r^2 = 0.9$; Fig. 4e).

**Heparin and tPA dose responses** Four coagulation parameters (TFCF, CR, RT, FFR) showed a strong linear correlation with heparin dose ($r^2$ between 0.71 and 0.99; Fig. 5b–e). Specifically, heparin had a significant effect on TFCF at a concentration as small as 0.15 U/mL (9.7 ± 1.2 min vs. 6.0 ± 0.15 min for the control group; Fig. 5b). TFCF for 0.225 U/mL and 0.3 U/mL heparin was 20 ± 1.6 min and 26 ± 5.5 min, respectively. CR and FFR decreased with the heparin dose, with a significant change from their normal values (3.1 ± 0.59°/min and 37 ± 1.6 $min^{-1}$) at 0.225 U/mL (1.1 ± 0.07°/min and 29 ± 1.3 $min^{-1}$) or 0.3 U/mL (0.71 ± 0.08°/min and 6.4 ± 0.33 $min^{-1}$) (Fig. 5c, e). RT also was significantly different from the normal plasma value (2.3 ± 0.20 min) at heparin concentration of 0.225 U/mL (5.7 ± 0.23 min) and 0.3 U/mL (6.9 ± 0.28 min) (Fig. 5d). CIT increased but showed insignificant difference between plasma without heparin (2.3 ± 0.52 min) and with 0.3 U/mL heparin (3.7 ± 0.50 min) (Fig. 5a). MCF and MFL changed insignificantly with heparin concentration between 0 and 0.3 U/mL (ESM Table S2). However, a decrease in clot firmness (MCF) was observed in whole blood for heparin concentrations greater than 1.0 U/mL (ESM Fig. S4a).

The effect of tPA-induced hyperfibrinolysis is clearly seen on mechanical tweezographs (Fig. 5f). LY10 linearly decreased with tPA concentration ($r^2 = 0.98$), with a significant difference between control (1.13 ± 0.005) and 0.5 mg/mL (1.07 ± 0.024) or 1.0 mg/mL tPA groups (1.03 ± 0.017) and between 0.1 mg/mL (1.09 ± 0.011) and 1.0 mg/mL tPA groups.

## Discussion

Results of this study indicate that acoustic tweezing technology can simultaneously measure turbidity and firmness of a single drop of blood devoid of red blood cells, e.g., platelet-poor or platelet-rich plasma. The integration of photo-optical measurements into QATT analysis [18] allowed for this technology to assess early stages of the coagulation cascade, such as fibrin formation, in addition to the late stage analysis (fibrin network formation and maturation) done by the QATT. This integrative noncontact approach, referred to as i-QATT™, enables rapid (<10 min) diagnosis and treatment monitoring of bleeding and thrombotic disorders and identification of coagulation factor deficiency. Due to small volume requirement, i-QATT™ analysis can be done on blood samples collected via finger or heal pricking [25–27]. The functional levels of fibrinogen and factor XIII can be measured directly from the MCF and MFL output.

One of the biggest advantages of i-QATT™ is its capability to monitor anticoagulant therapy, e.g., heparin therapy during major surgery [8, 28]. There is a strong linear correlation between heparin concentration and three coagulation parameters (RT, FFR, and TFCF). i-QATT™-based heparin therapy monitoring requires a small amount of blood that does not disturb blood circulation in a critical care patient.

Acoustic tweezing technology detects hyperfibrinolysis or the dose effect of fibrinolytic agents such as tPA at 10 to 15 min. tPA is produced endogenously by endothelial cells to accelerate the plasminogen-to-plasmin reaction, necessary for clot dissolution [29]. Recombinant tPA is an essential component of fibrinolytic therapy for patients with stroke or heart attack [30–32].

Using i-QATT™, the time delay between fibrin formation and clot maturation (FNFT) can be measured. FNFT uniquely depends on the functional level of FXIII, a fibrin cross-linker. When activated by thrombin, FXIII covalently binds the glutamine and lysine residues of forming fibrin strands, thus increasing clot firmness [33]. Patients with congenital FXIII deficiency (1–2% of the normal FXIII level) have serious

hemorrhagic complications such as intracranial hematoma. FXIII deficiency is often acquired, e.g., in pediatric malignancies [34], hyperfibrinolysis [35], and disseminated intravascular coagulation (DIC) [36, 37]. On the other hand, elevated FXIII levels contribute to the development of arterial and venous thrombosis [38]. Changes in FXIII activity cannot be measured by PT or aPTT tests, and the existing FXIII assays [39] are expensive and not readily available.

i-QATT™ addresses the issues of large sample volume and high variability of coagulation analyzers. Due to a minimum amount of blood sampled, this technology benefits neonatal and pediatric patients and adult patients with anemia or blood collection difficulties. Since both the device and sample are small in size, i-QATT™ can be used for rapid screening of coagulation abnormalities, e.g., in patients with infectious disease such as COVID-19, and for monitoring of anticoagulant therapy in outpatient settings or at home.

The next step in establishing clinical utility of i-QATT™ is to expand it to whole-blood analysis. While QATT itself works with whole blood, our photo-optical method is designed for blood plasma. Red blood cells abundantly present in whole blood mask the optical signal coming from fibrin molecules at wavelengths above 600 nm. Recent data obtained by UV-visible spectrophotometry [40, 41] and multi-wavelength light scattering [42] indicate that fibrin formation can be detected from the absorption spectrum, particularly, from absorbance at wavelengths of 350 nm and 600 to 800 nm where the contribution of red blood cells becomes relatively small. The implementation of the light absorption technique will be the focus of our future studies.

**Supplementary Information** The online version contains supplementary material available at https://doi.org/10.1007/s00216-021-03278-8.

**Acknowledgements** The authors thank R. Glynn Holt for help with the experimental system design and Nathan Nelson for fruitful discussion.

**Authors' contributions** D. Luo designed the study and the acoustic tweezing system, performed experiments, analyzed the data, and wrote the manuscript. M. Beard performed the fibrinogen, heparin, and tPA experiments. E. Chelales analyzed the data, helped with the code development, and performed factor deficiency plasma experiments. N. Kasireddy developed the data analysis code. D. Khismatullin conceived, designed, and supervised the study and wrote the manuscript.

**Funding** This study was supported by U.S. National Science Foundation grants No. 1438537 and 1725033 (to D.K.), U.S. National Science Foundation grant No. 1843479 (to. D.L), American Heart Association grant No. 13GRNT17200013 (to D.K.), and U.S. National Institutes of Health grant No. GM104940 (to Tulane University).

**Data availability** All the information about acoustic tweezing technology including the description of the methods to generate blood coagulation data is proprietary. However, the clinical data produced using this technology, such as graphical outputs ("tweezographs") and values of coagulation parameters, is available to the public. If accepted for publication, this manuscript will be submitted to the digital archive PubMed Central for sharing with general public, according to the NIH Public Access Policy.

**Code availability** Not applicable

## Declarations

**Conflict of interest** D. Luo, N. Kasireddy, and D. Khismatullin have a financial interest in Levisonics Inc. The other authors have no competing interests. i-QATT™ technology is protected by two pending patents: PCT/US14/55559 and PCT/US2018/014879.

**Ethics approval** Not applicable

**Consent to participate** Not applicable

**Consent for publication** Not applicable

## References

1. Herbstreit F, Winter EM, Peters J, Hartmann M. Monitoring of haemostasis in liver transplantation: comparison of laboratory based and point of care tests. Anaesthesia. 2010;65(1):44–9.
2. Levi M, Hunt BJ. A critical appraisal of point-of-care coagulation testing in critically ill patients. J Thromb Haemost. 2015;13(11):1960–7.
3. Chitlur M, Young G. Global assays in hemophilia. Semin Hematol. 2016;53(1):40–5.
4. Jennings I, Cooper P. Screening for thrombophilia: a laboratory perspective. Br J Biomed Sci. 2003;60(1):39–51.
5. Salmela B, Joutsi-Korhonen L, Armstrong E, Lassila R. Active online assessment of patients using new oral anticoagulants: bleeding risk, compliance, and coagulation analysis. Semin Thromb Hemost. 2012;38(1):23–30.
6. Taralov S, Kukladgiev B. Nephelometric study of the clotting of blood plasma (fibrinogen-fibrin phase) by patients with delirium tremens and chronic alcoholics. Folia Med (Plovdiv). 1976;18(2):171–6.
7. Koepke JA. Technologies for coagulation instruments. Lab Med. 2000;31(4):211–6.
8. Chen A, Teruya J. Global hemostasis testing thromboelastography: old technology, new applications. Clin Lab Med. 2009;29(2):391–407.
9. Durila M, Malosek M. Rotational thromboelastometry along with thromboelastography plays a critical role in the management of traumatic bleeding. Am J Emerg Med. 2014;32(3):288 e1–3.
10. Wang JS, Lin CY, Hung WT, O'Connor MF, Thisted RA, Lee BK, et al. Thromboelastogram fails to predict postoperative hemorrhage in cardiac patients. Ann Thorac Surg. 1992;53(3):435–9.
11. Ganter MT, Hofer CK. Coagulation monitoring: current techniques and clinical use of viscoelastic point-of-care coagulation devices. Anesth Analg. 2008;106(5):1366–75.
12. Chuang J, Sadler MA, Witt DM. Impact of evacuated collection tube fill volume and mixing on routine coagulation testing using 2.5-ml (pediatric) tubes. Chest. 2004;126(4):1262–6.
13. Pruthi RK. Abnormal partial thromboplast in time in adults and children. Clin Adv Hematol Oncol. 2011;9(6):466–7.

14. Lippi G, Favaloro EJ, Salvagno GL, Franchini M. Laboratory assessment and perioperative management of patients on antiplatelet therapy: from the bench to the bedside. Clin Chim Acta. 2009;405(1–2):8–16.
15. Capoor MN, Stonemetz JL, Baird JC, Ahmed FS, Awan A, Birkenmaier C, et al. Prothrombin time and activated partial thromboplastin time testing: a comparative effectiveness study in a million-patient sample. PLoS One. 2015;10(8):e0133317.
16. Tripodi A, Mannucci PM. The coagulopathy of chronic liver disease. N Engl J Med. 2011;365(2):147–56.
17. Pollack CV Jr. Coagulation assessment with the new generation of oral anticoagulants. Emerg Med J. 2016;33(6):423–30.
18. Holt RG, Luo D, Gruver N, Khismatullin DB. Quasi-static acoustic tweezing thromboelastometry. J Thromb Haemost. 2017;15(7):1453–62.
19. Ansari Hosseinzadeh V, Brugnara C, Emani S, Khismatullin D, Holt RG. Monitoring of blood coagulation with non-contact drop oscillation rheometry. J Thromb Haemost. 2019;17(8):1345–53.
20. Jeger V, Zimmermann H, Exadaktylos AK. Can RapidTEG accelerate the search for coagulopathies in the patient with multiple injuries? J Trauma Acute Care Surg. 2009;66(4):1253–7.
21. Brill-Edwards P, Ginsberg JS, Johnston M, Hirsh J. Establishing a therapeutic range for heparin therapy. Ann Intern Med. 1993;119(2):104–9.
22. Toulon P, Boutiere B, Horellou MH, Trzeciak MC, Samama MM. Monitoring heparin therapy using activated partial thromboplastin time–results of a multicenter trial establishing the therapeutic range for SILIMAT, a reagent with high sensitivity to heparin. Thromb Haemost. 1998;80(1):104–8.
23. Tyler HM. Fibrin crosslinking demonstrated by thrombelastography. Thromb Diath Haemorrh. 1969;22(2):398–400.
24. Carroll RC, Craft RM, Chavez JJ, Snider CC, Kirby RK, Cohen E. Measurement of functional fibrinogen levels using the thrombelastograph. J Clin Anesth. 2008;20(3):186–90.
25. Im SB, Kim SC, Shim JS. A smart pipette for equipment-free separation and delivery of plasma for on-site whole blood analysis. Anal Bioanal Chem. 2016;408(5):1391–7.
26. Kuo J-N, Zhan Y-H. Microfluidic chip for rapid and automatic extraction of plasma from whole human blood. Microsyst Technol. 2015;21(1):255–61.
27. Maria MS, Rakesh PE, Chandra TS, Sen AK. Capillary flow-driven microfluidic device with wettability gradient and sedimentation effects for blood plasma separation. Sci Rep. 2017;7:43457.
28. Zavadil DP, Stammers AH, Willett LD, Deptula JJ, Christensen KA, Sydzyik RT. Hematological abnormalities in neonatal patients treated with extracorporeal membrane oxygenation (ECMO). J Extra Corpor Technol. 1998;30(2):83–90.
29. Hoylaerts M, Rijken D, Lijnen H, Collen D. Kinetics of the activation of plasminogen by human tissue plasminogen activator. Role of fibrin. J Biol Chem. 1982;257(6):2912–9.
30. Lo EH, Broderick JP, Moskowitz MA. tPA and proteolysis in the neurovascular unit. Stroke. 2004;35(2):354–6.
31. Adibhatla RM, Hatcher JF. Tissue plasminogen activator (tPA) and matrix metalloproteinases in the pathogenesis of stroke: therapeutic strategies. CNS Neurol Disord Drug Targets. 2008;7(3):243–53.
32. Goldstein LB. Acute ischemic stroke treatment in 2007. Circulation. 2007;116(13):1504–14.
33. Loewy AG, College H (2001) Structure and function of factor XIII
34. Wiegering V, Andres O, Schlegel PG, Deinlein F, Eyrich M, Sturm A. Hyperfibrinolysis and acquired factor XIII deficiency in newly diagnosed pediatric malignancies. Haematologica. 2013;98:e90–1.
35. Dirkmann D, Gorlinger K, Gisbertz C, Dusse F, Peters J. Factor XIII and tranexamic acid but not recombinant factor VIIa attenuate tissue plasminogen activator-induced hyperfibrinolysis in human whole blood. Anesth Analg. 2012;114(6):1182–8.
36. Rodeghiero F, Barbui T, Battista R, Chisesi T, Rigoni G, Dini E. Molecular subunits and transamidase activity of factor XIII during disseminated intravascular coagulation in acute leukaemia. Thromb Haemost. 1980;43(01):006–9.
37. Song JW, Choi JR, Song KS, Rhee JH. Plasma factor XIII activity in patients with disseminated intravascular coagulation. Yonsei Med J. 2006;47(2):196–200.
38. Muszbek L, Bagoly Z, Bereczky Z, Katona E. The involvement of blood coagulation factor XIII in fibrinolysis and thrombosis. Cardiovasc Hematol Agents Med Chem. 2008;6(3):190–205.
39. Dorgalaleh A, Kazemi A, Zaker F, Shamsizadeh M, Rashidpanah J, Mollaei M. Laboratory diagnosis of factor XIII deficiency, routine coagulation tests with quantitative and qualitative methods. Clin Lab. 2016;62(4):491–8.
40. Chernysh IN, Weisel JW. Dynamic imaging of fibrin network formation correlated with other measures of polymerization. Blood. 2008;111(10):4854–61.
41. Wiman B, Ranby M. Determination of soluble fibrin in plasma by a rapid and quantitative spectrophotometric assay. Thromb Haemost. 1986;55(2):189–93.
42. Dassi C, Seyve L, Garcia X, Bigo E, Marlu R, Caton F, et al. Fibrinography: a multiwavelength light-scattering assay of fibrin structure. Hemasphere. 2019;3(1):e166.